J Musculoskelet Neuronal Interact 2025; 25(3):341-350

Journal of Musculoskeletal and Neuronal Interactions JMNI

Original Article

In Vivo and *In Vitro* Analysis of Cathepsin D in Bone Homeostasis and Osteoporosis

Song Yan[1,2], Jiancong Zeng[1,2], Wei Dong[2], Jinsong Wei[3]

[1]The First Clinical Medical College of Guangdong Medical University, Zhanjiang, China;
[2]Department of Orthopedics, Shiyan People's Hospital, Bao'an District, Shenzhen, China;
[3]Department of Spinal Degeneration and Deformity Surgery, Affiliated Hospital of Guangdong Medical University, Zhanjiang, China

Abstract

Objectives: To explore the role of cathepsin D (CTSD), a lysosomal aspartyl protease, as a potential biomarker and therapeutic target in the context of osteoporosis. **Methods**: Utilizing single-cell sequencing data from the Gene Expression Omnibus (GEO) database, we identified differential expression patterns of CTSD in human femoral head tissues between osteoporotic and non-osteoporotic states. Human mesenchymal stem cells (MSCs) were treated with recombinant human CTSD and/or osteogenic induction medium and the role of CTSD on osteoblast differentiation were investigated by RT-qPCR, western blot, immunofluorescence staining and alizarin red staining. The role of CTSD on osteoporotic changes was further verified in ovariectomized mice. **Results**: *In vitro* analyses of human mesenchymal stem cells (MSCs) treated with recombinant human CTSD (rhCTSD) under osteogenic induction conditions revealed modulation of osteogenic marker expression, including ALP, COL1A1, and RUNX2. Histological assessments using Alizarin Red staining and immunofluorescence corroborated these findings, demonstrating that CTSD influences osteoblast differentiation and matrix mineralization. *In vivo* studies in mice further supported the role of CTSD, showing that perturbations in this enzyme result in alterations in bone mineral density and volume characteristic of osteoporotic changes. **Conclusion**: Collectively, these findings implicate CTSD as a regulator of bone homeostasis and support its potential as a novel target for therapeutic intervention in osteoporosis.

Keywords: Biomarkers, Bone Remodeling, Cathepsin D, CTSD, Osteoporosis

Introduction

Osteoporosis is a common skeletal disorder characterized by reduced bone mass and deterioration of bone tissue, leading to increased bone fragility and susceptibility to fractures. The condition is typically identified by decreased bone mineral density (BMD), which compromises skeletal strength and increases the risk of serious health complications[1,2]. Both men and women are at risk of osteoporotic fractures, with advancing age being a major contributing factor[3,4]. Due to hormonal changes, particularly estrogen deficiency, postmenopausal women experience a significantly higher incidence of osteoporosis[5–7]. Globally, osteoporosis imposes a substantial economic burden, primarily due to the high costs associated with the treatment of osteoporosis-related fractures[8,9].

Cellular aging is closely associated with osteoporosis, although the underlying molecular mechanisms and therapeutic targets involved in these cellular changes remain largely unexplored[10]. Emerging evidence suggests that various forms of regulated cell death, including necroptosis[11], ferroptosis[12], and the involvement of fibrotic proteins[13] and pathways such as HO-1[14], contribute to the pathogenesis of osteoporosis. Among the critical genes identified in osteoporosis-related datasets, cathepsin D (CTSD) has been highlighted as a potential biomarker for postmenopausal osteoporosis[15–17]. CTSD is a lysosomal aspartyl protease[18,19], predominantly expressed in its inactive proenzyme form (pro-CTSD) in humans[20]. It is found in various tissues throughout the body[21–23], where it plays diverse roles, including the regulation of apoptosis[24], promotion of cell proliferation[25], and involvement in tumor progression[23,26]. Although CTSD has been identified as differentially expressed in osteoporosis, its specific role and

The authors have no conflict of interest.

Corresponding author: Jinsong Wei, Department of Spinal Degeneration and Deformity Surgery, Affiliated Hospital of Guangdong Medical University, No. 57, South Renmin Avenue, Xiashan District, Zhanjiang 524001, Guangdong Province, China
E-mail: jinsong.wei@gdmu.edu.cn

Edited by: G. Lyritis
Accepted 13 March 2025

effects on bone cells remain poorly understood.

Osteoporosis is a disease characterized by an imbalance between osteoclast and osteoblast activity, leading to impaired bone remodeling and increased fracture risk[27,28]. Investigating therapeutic gene targets is a critical aspect of osteoporosis research. The aim of this study was to examine the potential role of CTSD in the osteogenic differentiation of mesenchymal stem cells (MSCs), as well as its effects on bone physiology in mice.

Materials and methods

Data Collection

The dataset GSE147287 was obtained from the Gene Expression Omnibus (GEO) and contains single-cell RNA sequencing data from non-osteoporotic and osteoporotic human femoral tissue samples).

Cell Culture and Intervention

Human mesenchymal stem cells (MSCs) (HUM-iCell-s011, iCell Bioscience Inc., China) used in this study were obtained from a certified commercial source and handled according to the manufacturer's ethical and usage guidelines. No human subjects or personally identifiable information were involved. The culture medium was human MSC complete medium (CM-H166-100, Procell Inc., China). For all subsequent procedures, cells were cultured in an incubator maintained at 37°C with 5% CO_2 after reaching passage 2. Passaged cells were seeded into flasks and allowed to adhere in the incubator. Once the cell density reached 50%–70%, the following treatments were applied: control medium, recombinant human cathepsin D (rhCTSD; HY-P7748A, MCE), osteogenic induction medium (OIM; PD-003, Procell, China), and a combination of rhCTSD and OIM. Cells were harvested either after 7 days of OIM treatment or 24 hours of rhCTSD exposure[29–31]. The effective concentration of rhCTSD used in the culture experiments was 20 μg/mL[29].

Gene expression variations in cells were identified by RT-qPCR analysis

Gene expression variations induced by rhCTSD and OIM in human MSCs were analyzed using RT-qPCR. Human MSCs were treated with OIM for 7 days or with rhCTSD for 24 hours. RT-qPCR was performed to evaluate the expression levels of ALP, COL1A1, CTSD, and RUNX2 in each experimental group. Differential gene expression in osteogenically induced and CTSD-treated cells was assessed by analyzing changes in target gene levels following treatment. mRNA expression was quantified using the 2^−ΔΔCt method, with GAPDH used as an endogenous control.

Primer sequences were as follows:

- ALP-F: 5′-ACCAGGATTACACCAGGAAGCAAG-3′; ALP-R: 5′-ACTCTGTCCCAAAGCCGTCAATAG-3′
- COL1A1-F: 5′-AAAGATGGACTCAACGGTCTC-3′; COL1A1-R: 5′-CATCGTGAGCCTTCTCTTGAG-3′
- CTSD-F: 5′-ACAACAACAGCGACAAGTCCAGCAC-3′; CTSD-R: 5′-TGGCAGGGCACCGACACACAG-3′
- RUNX2-F: 5′-AGGCAGTTCCCAAGCATTTCATCC-3′; RUNX2-R: 5′-TGGCAGGTAGGTGTGGTAGTGAG-3′
- GAPDH-F: 5′-GTCTCCTCTGACTTCAGCG-3′; GAPDH-R: 5′-ACCACCCTGTTGGTAGCCAA-3′

Western Blot Analysis of Protein Expression

Cells from each experimental group were rinsed twice with PBS and lysed in RIPA buffer (R0010, Solarbio) containing 1% phenylmethanesulfonyl fluoride (PMSF) for 10 minutes. Lysates were centrifuged at 15,000 × g for 10 minutes at 4°C, and protein concentrations were determined using a BCA protein assay kit (P0010, Beyotime). Equal amounts of protein were separated on 12.5% SDS-PAGE gels and transferred to PVDF membranes (TM-PVDF-R-45, LABSELECT). Membranes were blocked with Western blocking solution (P0023B, Beyotime) for 90 minutes at room temperature and then incubated overnight at 4°C with the following primary antibodies: anti-ALPL (11187-1-AP, Proteintech), anti-RUNX2 (SEM29595, SAB), anti-CTSD (ab75811, Abcam), anti-COL1A1 (AF7001, Affinity), and anti-GAPDH (AF7021, Affinity). After washing, membranes were incubated with HRP-conjugated secondary antibody (LF102, EpiZyme) for 1 hour at room temperature. Protein bands were visualized using the BeyoECL Plus chemiluminescence system (P0018FM, Beyotime), and band intensities were quantified using ImageJ software (version 1.8.0).

Immunofluorescence Staining

Prior to immunofluorescence analysis, cells were divided into three experimental groups: control, OIM-induced, and OIM plus rhCTSD co-culture groups. After reaching the designated incubation time, cells were resuspended in culture medium at a density of 5×10^5 cells/mL. Cells were then fixed with 4% paraformaldehyde (PFA) for 20 minutes, followed by permeabilization with 0.5% Triton X-100 for 20 minutes. Non-specific binding was blocked using 5% bovine serum albumin (BSA) for 10 minutes at room temperature. Cells were incubated overnight at 4°C with an ALP-specific primary antibody (11187-1-AP, Proteintech Group), followed by incubation with a secondary antibody for 1 hour at room temperature. Slides were mounted using antifade mounting medium (BY-1002), which preserved DAPI (4′,6-diamidino-2-phenylindole) nuclear staining. Images were acquired using a Zeiss LSM 880 confocal microscope.

Alizarin Red Staining

Alizarin red staining was performed according to standard protocols. Cells were first rinsed with phosphate-buffered saline (PBS) and then fixed with 95% ethanol for 10 minutes. To detect mineralized nodules, cells were incubated with 0.1% alizarin red S solution (G1450, Solarbio) for 10 minutes. Stained mineral deposits were examined and

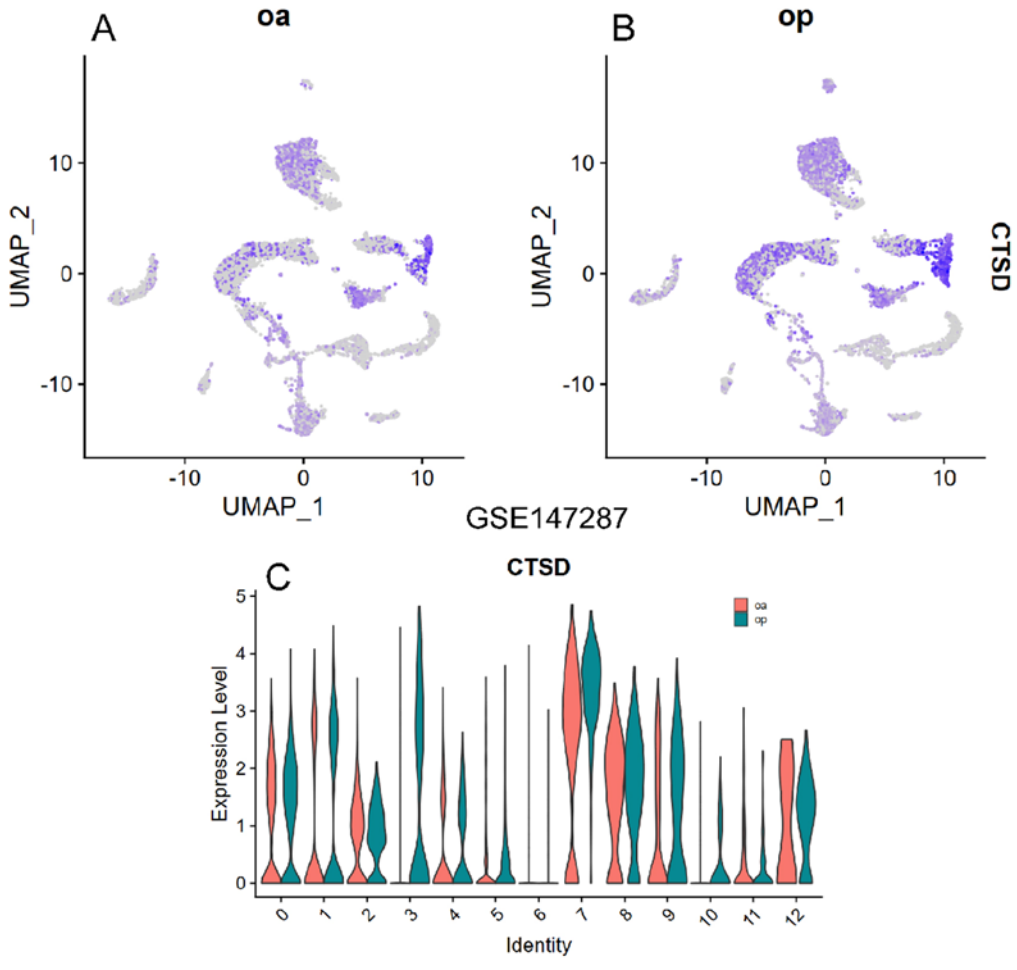

Figure 1. (A) UMAP plots showing the distribution of CTSD expression in osteoporosis (OP) and osteoarthritis (OA) samples from the database. (B) Violin plots comparing CTSD expression levels between OP and OA samples.

documented using light microscopy. For quantification, the bound dye was extracted, and absorbance was measured at 570 nm using a plate reader, providing an objective assessment of mineralization levels in each group.

Immunohistochemistry Analysis

Immunohistochemistry was performed to detect ALP protein expression in MSC, which were initially plated in a 6-well plate at a density of 1×10^4 cells per well. Cells were divided into two experimental groups: an OIM-induced group and an OIM plus rhCTSD co-culture group. After the co-culture reached the designated time point, cells were resuspended in culture medium at a density of 5×10^5 cells/mL. Following post-fixation in 4% paraformaldehyde for 30 minutes, the slides were blocked with goat serum to prevent non-specific antibody binding. Slides were then incubated overnight at 4°C with an ALP-specific primary antibody (11187-1-AP, Proteintech Group). The following day, slides were incubated with an ALP-conjugated secondary antibody at a 1:50 dilution for 30 minutes at room temperature. Finally, stained cells were examined and imaged under a light microscope.

Animal Experiments

Nine 8-week-old male C57BL/6 mice (Changsheng Biotechnology) were randomly assigned to three groups: blank control, ovariectomized (OVX), and CTSD intraperitoneal injection (CTSD-Ip) groups. All mice were fed the same standard diet (YC-FOO1, Changsheng Biotechnology). In the OVX group, bilateral ovariectomy was performed at 8 weeks of age, and mice recovered well postoperatively[32,33]. In the CTSD-Ip group, mice received one intraperitoneal injection of rhCTSD (50 mg/kg) at 8 weeks of age, followed by four additional intraperitoneal injections of 25 mg/kg (twice per week for 2 weeks), and a final injection of 25 mg/kg via the tail vein at 11 weeks of age[29]. All mice were housed under standard conditions and allowed free access to food and water. After 28 days of

treatment, animals were euthanized by cervical dislocation under ether anesthesia. No mortality was observed during the experimental period. After euthanasia under ether anesthesia, bilateral femurs were harvested and stored in tissue preservation solution at −20°C for subsequent micro-CT analysis.

Micro-CT Analysis

Hip joints were fixed in 4% paraformaldehyde for 48 hours, then washed with phosphate-buffered saline (PBS) and stored in 75% ethanol. Microstructural analysis was performed using a SkyScan 1176 micro-CT system (Bruker micro-CT, Bruker Belgium SA, Kontich, Belgium). Scanning was conducted on a 1 mm region of metaphyseal trabecular bone in the distal femur, located 0.5 mm above the growth plate, to evaluate bone microarchitecture. Three-dimensional image reconstruction and realignment were performed using NRecon and CTAn software (version 1.17.7.2, Bruker).

Statistical analysis

Clustering, identification of differentially expressed genes, and detection of marker genes within single-cell populations—were conducted using R software (version 4.2.0) and the Seurat package (version 4.0), developed by the Satija Lab. Data in the experiments were repeated in biological triplicates, represented as mean ± standard deviation and histograms were generated using GraphPad Prism software (version 8.0). Statistical significance was compared by Student's *t* test or one-way analysis of variance with Tukey's method when applicable. Statistical significance was defined as a P value less than 0.05 ($P < 0.05$).

Results

Differential Expression of CTSD in Human Osteoporotic and Non-Osteoporotic Bone Samples

Analysis of the GSE147287 dataset from theGEO database revealed significant differences in CTSD gene expression between osteoporotic and non-osteoporotic human femoral head tissue samples (Figure 1A, B). CTSD was also found to be differentially expressed across various cell types within both sample groups (Figure 1C).

Gene Expression Changes in Human MSCs Following Osteogenic Induction and rhCTSD Treatment

Successful osteogenic induction of human MSCs was confirmed by the upregulation of ALP, COL1A1, and RUNX2 following treatment with OIM. To investigate the role of CTSD in osteoblast differentiation, gene expression was analyzed in the MSC-OIM-rhCTSD experimental group. In this group, the expression of ALP, COL1A1, and RUNX2 was found to decrease to varying degrees after rhCTSD treatment, suggesting an inhibitory effect on osteogenesis. However, treatment with rhCTSD alone did not result in statistically significant changes in the expression of these markers (Figure 2).

Quantitative Analysis of Protein Expression Changes in MSCs Treated with rhCTSD During Osteogenic Induction

Western blot analysis was performed to assess protein expression after 48 hours of treatment in four groups: MSC (n = 3), MSC-rhCTSD (n = 3), MSC-OIM-rhCTSD (n = 3), and MSC-OIM (n = 3) (Figure 3). Compared with the control group, the expression levels of COL1A1, ALP, and RUNX2 were elevated in MSCs induced with osteogenic induction medium (OIM), consistent with RT-qPCR results, confirming successful osteogenesis. However, in cells treated with both OIM and rhCTSD, the expression levels of these osteogenic markers were reduced. Notably, only CTSD expression was upregulated in response to rhCTSD treatment.

Immunofluorescence Detection of ALPL Expression Following CTSD Intervention

Immunofluorescence staining was used to evaluate ALPL expression in MSC (n = 3), MSC-OIM (n = 3), and MSC-OIM-rhCTSD (n = 3) groups after 48 hours of treatment (Figure 4). Cells in the OIM group showed increased ALPL fluorescence intensity, indicating enhanced osteogenic differentiation. However, ALPL expression was reduced in the MSC-OIM-rhCTSD group compared to the MSC-OIM group, suggesting that rhCTSD may suppress ALPL expression during osteogenesis.

Alizarin Red Staining to Evaluate Mineralization Potential

Alizarin Red staining was performed to assess the mineralization capacity of MSCs under different treatment conditions (Figure 5). Cells treated with OIM exhibited a higher degree of mineral deposition compared to untreated MSCs, indicating effective osteogenic differentiation. In contrast, the MSC-OIM-rhCTSD group showed markedly reduced mineralization compared to the OIM-only group, suggesting that rhCTSD negatively affects the mineralization ability of differentiating osteoblasts.

Immunohistochemical Detection of ALPL Expression Following rhCTSD Intervention

Immunohistochemical staining was used to evaluate ALPL expression in the experimental groups (Figure 6). Brown chromogenic labeling indicated the presence of ALPL, which was primarily localized in the cytoplasm. In the MSC-OIM-rhCTSD group, ALPL staining intensity was reduced, suggesting downregulation of ALPL expression under rhCTSD intervention. In contrast, the MSC-OIM group showed stronger ALPL staining, consistent with enhanced osteogenic activity.

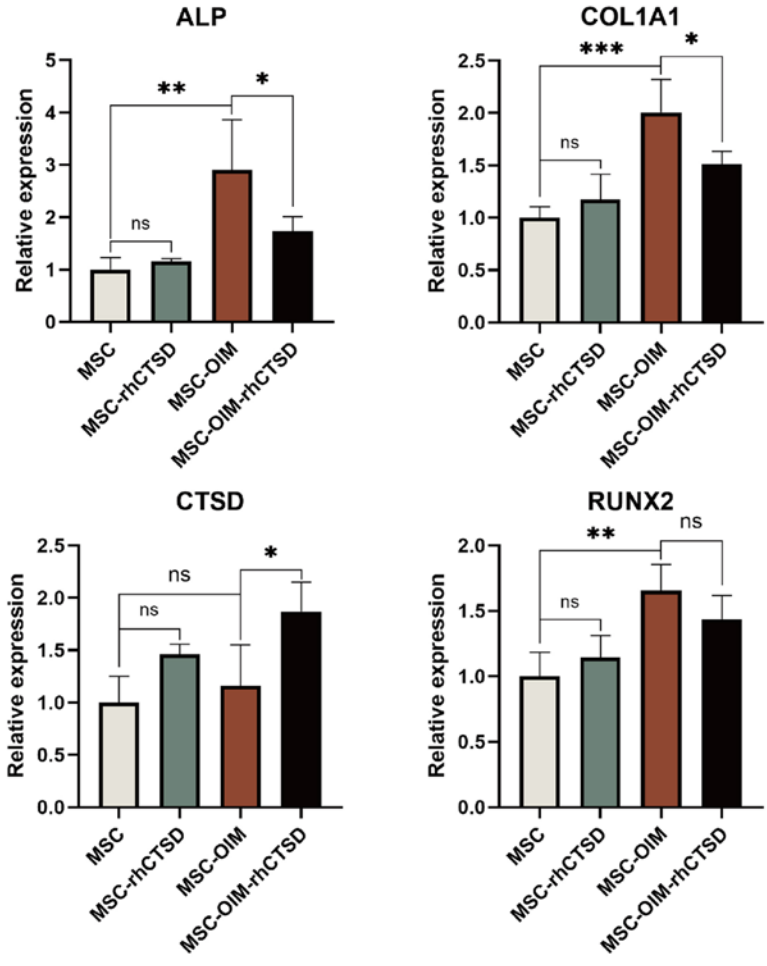

Figure 2. Gene expression levels in MSCs treated under each experimental condition, as determined by RT-qPCR. ($p < 0.05$, $p < 0.01$, $p < 0.001$, $p < 0.0001$; ns indicates no statistically significant difference.)

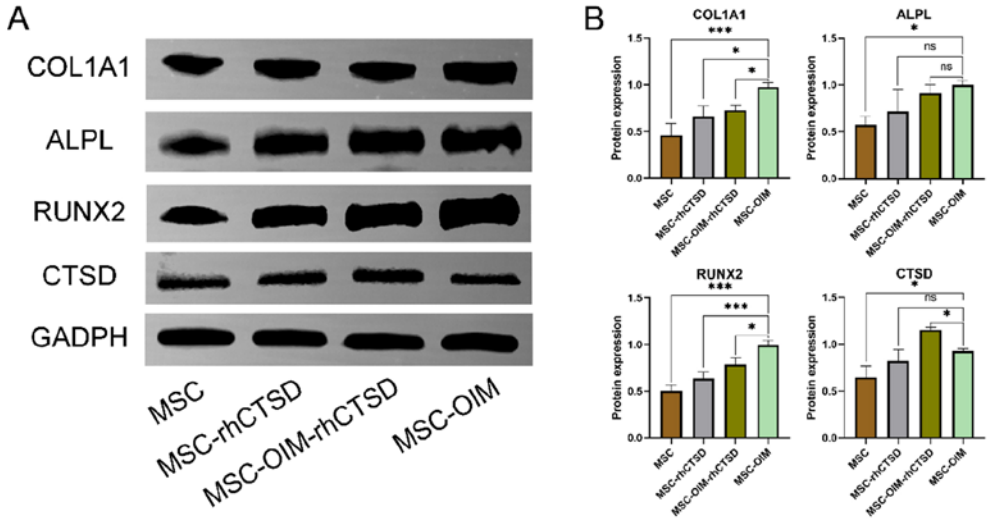

Figure 3. Western blot analysis of protein expression levels across different experimental groups. ($p < 0.05$, $p < 0.01$, $p < 0.001$; ns indicates no statistically significant difference).

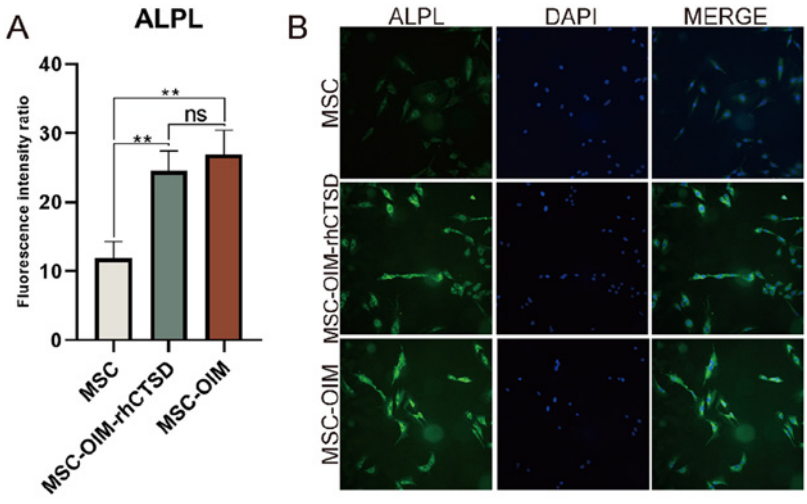

Figure 4. Immunofluorescence staining showing ALPL expression in nucleus pulposus cells from each experimental group. ($p < 0.01$; ns indicates no statistically significant difference).

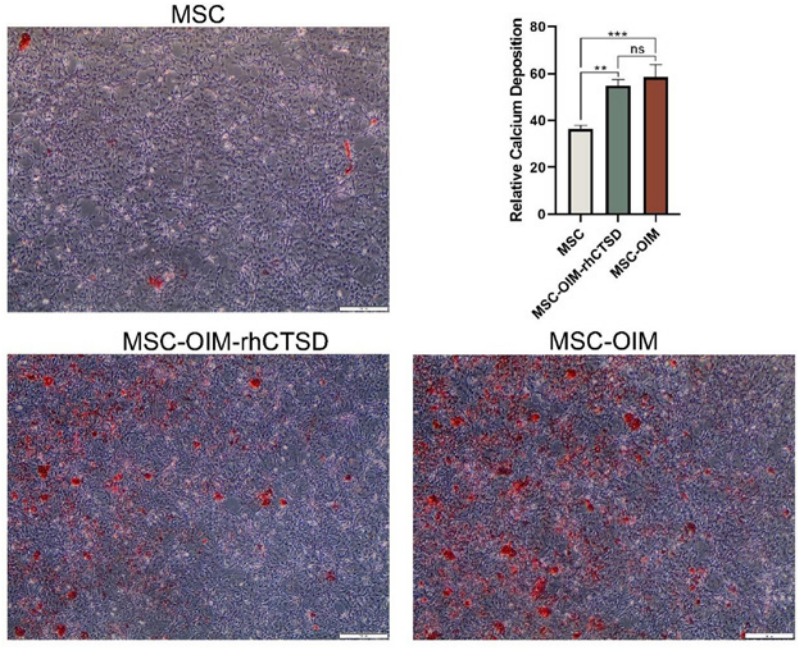

Figure 5. Alizarin Red staining was used to assess mineralization capacity in each group. ($p < 0.01$, $p < 0.001$; ns indicates no statistically significant difference).

Effect of CTSD on the Hip Joint of Mice

Mice were divided into three groups: control, OVX, and CTSD intraperitoneal injection (CTSD-Ip). Micro-CT analysis was performed on the proximal femur after the completion of treatment and feeding (Figure 7A). The OVX group exhibited reduced BMD and a lower bone volume-to-total volume ratio (BV/TV) compared to the control group, indicating bone loss due to estrogen deficiency. Similarly, the CTSD-Ip group showed decreased BMD and BV/TV to varying degrees compared to the control group (Figure 7B), suggesting that rhCTSD may contribute to bone deterioration *in vivo*.

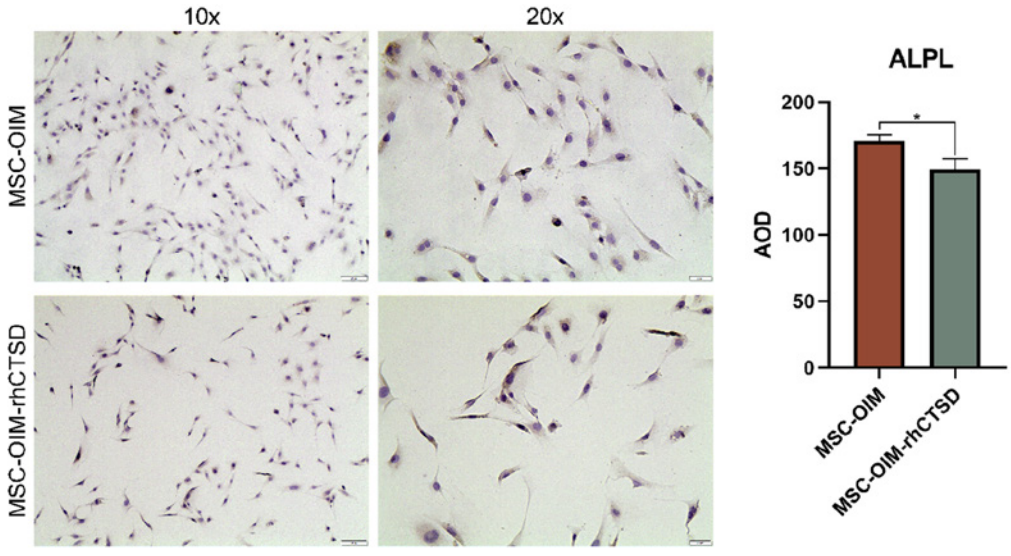

Figure 6. Immunohistochemical staining of alkaline phosphatase (ALPL) expression in experimental groups, ($p < 0.05$).

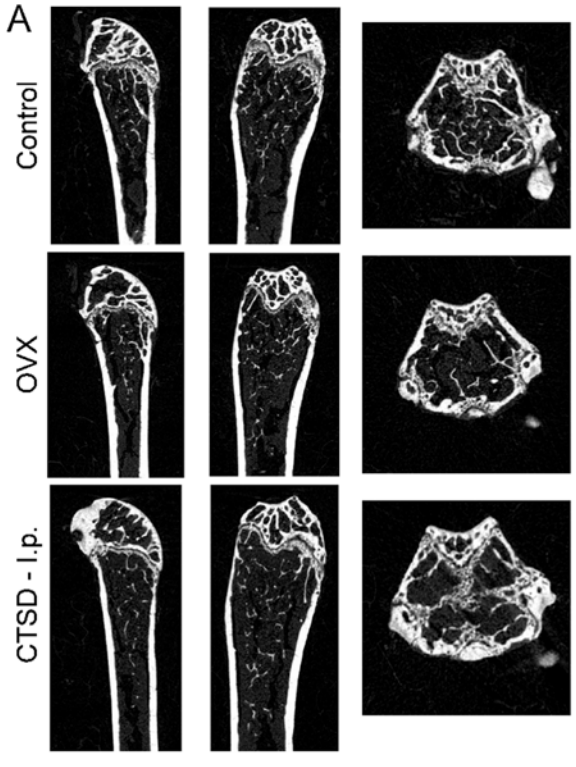

B

	BMD(g/cm3)	BV/TV(%)	Tb.N(1/mm)	Tb.Sp(mm)	Tb.Th(mm)	SMI
Control	0.47046	19.77287	0.12856	0.51598	1.55148	-0.97570
OVX	-0.03596	14.95939	0.13072	0.73547	1.15448	-0.99717
CTSD - I.p.	0.07950	18.79172	0.13301	0.56888	1.42472	-1.07642

Figure 7. Micro-CT analysis of the effects of CTSD treatment in mice. (A) Sagittal, coronal, and axial views of the femoral heads from each experimental group. (B) Quantitative evaluation of bone parameters, including femoral bone mineral density (BMD) and other microstructural metrics.

Discussion

In previous mechanistic studies investigating homeostatic imbalances in bone remodeling associated with osteoporosis, several therapeutic strategies have been developed based on well-established molecular pathways[35]. Among the most commonly used treatments are bisphosphonates, which inhibit bone resorption by preventing the breakdown of hydroxyapatite[36], and denosumab, a monoclonal antibody that targets RANKL (receptor activator of nuclear factor-κB ligand) to suppress osteoclast activity and slow bone degradation[37]. Although these therapies are effective, they are associated with significant limitations and adverse effects, including osteonecrosis of the jaw and atypical fractures[38]. Therefore, it remains critical to further investigate the molecular mechanisms underlying osteoporosis and to identify novel therapeutic targets for its prevention and treatment.

Cathepsin D (CTSD) is a lysosomal aspartyl protease that has been shown to regulate apoptosis and cell proliferation in mammals[39,40]. Research suggests that the tissue-specific expression of CTSD plays a critical role in determining developmental outcomes[41]. Recent studies have indicated that CTSD may be involved in the molecular mechanisms underlying osteoporosis progression[16,17] and has the potential to serve as a biomarker for the disease[15]. However, the specific effects of CTSD on bone cells, as well as the underlying biological mechanisms through which it contributes to osteoporosis, remain unclear and warrant further investigation.

In this study, we investigated differences in CTSD expression between osteoporotic and non-osteoporotic human bone tissue samples, as well as its potential biological effects. Differential expression of CTSD was initially identified through analysis of bioinformatics data and subsequently confirmed through experimental validation. A combination of qRT-PCR, Western blotting, immunofluorescence, immunohistochemistry, and Alizarin Red staining revealed that upregulation of CTSD altered the expression of osteogenic markers ALP, RUNX2, and COL1A1 in osteoblasts. These results suggest that CTSD may contribute to disrupted bone homeostasis in osteoporosis. Furthermore, *in vivo* experiments demonstrated that BMD and bone volume were reduced to varying degrees following intraperitoneal and intravenous administration of rhCTSD in mice. These changes closely resembled those observed in OVX osteoporotic model mice.

Together, these findings offer preliminary insights into the possible role of CTSD in the pathogenesis of osteoporosis and suggest its potential as a candidate for further investigation as a therapeutic target. This study also provides early evidence of CTSD's involvement in bone cell function and bone structure in mice, which may inform the development of future therapeutic strategies. However, further research is necessary to explore the interactions of CTSD with components of the extracellular matrix and intracellular signaling pathways. Functional studies will be essential to validate its role and clarify its relevance in the context of osteoporosis.

Conclusion

In this study, we explored the potential role of CTSD in osteocyte function and osteogenesis within the context of osteoporosis. Our results suggest that CTSD expression may be associated with the regulation of key osteogenic markers, indicating its possible involvement in bone remodeling processes. While these findings offer preliminary insights into the pathogenesis of osteoporosis, further research is needed to clarify the functional role of CTSD and to assess its potential as a therapeutic target.

Ethics approval

All animal procedures were approved by the Animal Care and Use Committee of the Affiliated Hospital of Guangdong Medical University (Approval Number: No. PJKT2022-046). Commercially obtained human MSCs were used in accordance with supplier guidelines. No additional human subjects were involved. Publicly available data from the GEO database (GSE147287) were used in compliance with database terms and conditions.

Authors' contributions

Writing – original draft preparation, software, validation, formal analysis: Song Yan, Jiancong Zeng, Wei Dong. Resources, data curation: Wei Dong. Conceptualization, methodology, writing – review and editing: Song Yan, Jiancong Zeng, Jinsong Wei. Supervision, project administration, funding acquisition: Jinsong Wei. All authors have read and approved the final version of the manuscript.

Funding

This study was supported by Project initiated by high-level talent research in Affiliated Hospital of Guangdong Medical University (GCC2022007).

References

1. Song S, Guo Y, Yang Y, Fu D. Advances in pathogenesis and therapeutic strategies for osteoporosis. Pharmacol Ther. 2022;237:108168.
2. Armas LA, Recker RR. Pathophysiology of osteoporosis: new mechanistic insights. Endocrinol Metab Clin North Am. 2012;41(3):475-86.
3. Reid IR. Short-term and long-term effects of osteoporosis therapies. Nat Rev Endocrinol. 2015; 11(7):418-28.
4. Coughlan T, Dockery F. Osteoporosis and fracture risk in older people. Clin Med (Lond). 2014;14(2):187-91.
5. Rachner TD, Khosla S, Hofbauer LC. Osteoporosis: now and the future. Lancet. 2011;377(9773):1276-87.
6. Black DM, Rosen CJ. Clinical Practice. Postmenopausal Osteoporosis. N Engl J Med. 2016;374(3):254-62.
7. Chotiyarnwong P, McCloskey EV. Pathogenesis of glucocorticoid-induced osteoporosis and options for treatment. Nat Rev Endocrinol. 2020;16(8):437-447.

8. Burge R, Dawson-Hughes B, Solomon DH, Wong JB, King A, Tosteson A. Incidence and economic burden of osteoporosis-related fractures in the United States, 2005-2025. J Bone Miner Res. 2007;22(3):465-75.
9. Ström O, Borgström F, Kanis JA, Compston J, Cooper C, McCloskey EV, Jönsson B. Osteoporosis: burden, health care provision and opportunities in the EU: a report prepared in collaboration with the International Osteoporosis Foundation (IOF) and the European Federation of Pharmaceutical Industry Associations (EFPIA). Arch Osteoporos. 2011;6:59-155.
10. Wang T, Huang S, He C. Senescent cells: A therapeutic target for osteoporosis. Cell Prolif. 2022;55(12):e13323.
11. Hu X, Wang Z, Kong C, Wang Y, Zhu W, Wang W, Li Y, Wang W, Lu S. Necroptosis: A new target for prevention of osteoporosis. Front Endocrinol (Lausanne). 2022;13:1032614.
12. Gao Z, Chen Z, Xiong Z, Liu X. Ferroptosis - A new target of osteoporosis. Exp Gerontol. 2022;165:111836.
13. Starling S. New anti-osteoporosis drug target identified. Nat Rev Endocrinol. 2021;17(1):4-5.
14. Che J, Yang J, Zhao B, Shang P. HO-1: A new potential therapeutic target to combat osteoporosis. Eur J Pharmacol. 2021;906:174219.
15. Deng YX, He WG, Cai HJ, Jiang JH, Yang YY, Dan YR, Luo HH, Du Y, Chen L, He BC. Analysis and Validation of Hub Genes in Blood Monocytes of Postmenopausal Osteoporosis Patients. Front Endocrinol (Lausanne). 2022;12:815245.
16. Wang X, Pei Z, Hao T, Ariben J, Li S, He W, Kong X, Chang J, Zhao Z, Zhang B. Prognostic analysis and validation of diagnostic marker genes in patients with osteoporosis. Front Immunol. 2022;13:987937.
17. Mo L, Ma C, Wang Z, Li J, He W, Niu W, Chen Z, Zhou C, Liu Y. Integrated Bioinformatic Analysis of the Shared Molecular Mechanisms Between Osteoporosis and Atherosclerosis. Front Endocrinol (Lausanne). 2022;13:950030.
18. Stoka V, Turk V, Turk B. Lysosomal cathepsins and their regulation in aging and neurodegeneration. Ageing Res Rev. 2016;32:22-37.
19. Faust PL, Kornfeld S, Chirgwin JM. Cloning and sequence analysis of cDNA for human cathepsin D. Proc Natl Acad Sci U S A. 1985;82(15):4910-4.
20. Khalkhali-Ellis Z, Hendrix MJ. Two Faces of Cathepsin D: Physiological Guardian Angel and Pathological Demon. Biol Med (Aligarh). 2014;6(2):1000206.
21. Prieto Huarcaya S, Drobny A, Marques ARA, Di Spiezio A, Dobert JP, Balta D, Werner C, Rizo T, Gallwitz L, Bub S, Stojkovska I, Belur NR, Fogh J, Mazzulli JR, Xiang W, Fulzele A, Dejung M, Sauer M, Winner B, Rose-John S, Arnold P, Saftig P, Zunke F. Recombinant pro-CTSD (cathepsin D) enhances SNCA/α-Synuclein degradation in α-Synucleinopathy models. Autophagy. 2022;18(5):1127-1151.
22. Zhou Y, Huang X, Yu H, Shi H, Chen M, Song J, Tang W, Teng F, Li C, Yi L, Zhu X, Wang N, Wei Y, Wuniqiemu T, Dong J. TMT-based quantitative proteomics revealed protective efficacy of Icariside II against airway inflammation and remodeling via inhibiting LAMP2, CTSD and CTSS expression in OVA-induced chronic asthma mice. Phytomedicine. 2023;118:154941.
23. Ding P, Xu Y, Li L, Lv X, Li L, Chen J, Zhou D, Wang X, Wang Q, Zhang W, Liao T, Ji QH, Lei QY, Hu W. Intracellular complement C5a/C5aR1 stabilizes β-catenin to promote colorectal tumorigenesis. Cell Rep. 2022;39(9):110851.
24. Bröker LE, Kruyt FA, Giaccone G. Cell death independent of caspases: a review. Clin Cancer Res. 2005;11(9):3155-62.
25. Ohri SS, Vashishta A, Proctor M, Fusek M, Vetvicka V. The propeptide of cathepsin D increases proliferation, invasion and metastasis of breast cancer cells. Int J Oncol. 2008;32(2):491-8.
26. Ketterer S, Mitschke J, Ketscher A, Schlimpert M, Reichardt W, Baeuerle N, Hess ME, Metzger P, Boerries M, Peters C, Kammerer B, Brummer T, Steinberg F, Reinheckel T. Cathepsin D deficiency in mammary epithelium transiently stalls breast cancer by interference with mTORC1 signaling. Nat Commun. 2020;11(1):5133.
27. Cui Y, Lv B, Li Z, Ma C, Gui Z, Geng Y, Liu G, Sang L, Xu C, Min Q, Kong L, Zhang Z, Liu Y, Qi X, Fu D. Bone-Targeted Biomimetic Nanogels Re-Establish Osteoblast/Osteoclast Balance to Treat Postmenopausal Osteoporosis. Small. 2024;20(6):e2303494.
28. Kim JM, Lin C, Stavre Z, Greenblatt MB, Shim JH. Osteoblast-Osteoclast Communication and Bone Homeostasis. Cells. 2020;9(9):2073.
29. Marques ARA, Di Spiezio A, Thießen N, Schmidt L, Grötzinger J, Lüllmann-Rauch R, Damme M, Storck SE, Pietrzik CU, Fogh J, Bär J, Mikhaylova M, Glatzel M, Bassal M, Bartsch U, Saftig P. Enzyme replacement therapy with recombinant pro-CTSD (cathepsin D) corrects defective proteolysis and autophagy in neuronal ceroid lipofuscinosis. Autophagy. 2020;16(5):811-825.
30. Xing Y, Zhong X, Chen S, Wu S, Chen K, Li X, Su M, Liu X, Zhong J, Chen Z, Pan H, Chen Z, Liu Q. Optimized osteogenesis of porcine bone-derived xenograft through surface coating of magnesium-doped nanohydroxyapatite. Biomed Mater. 2023;18(5).
31. Zhu D, Peng T, Zhang Z, Guo S, Su Y, Zhang K, Wang J, Liu C. Mesenchymal stem cells overexpressing XIST induce macrophage M2 polarization and improve neural stem cell homeostatic microenvironment, alleviating spinal cord injury. J Tissue Eng. 2024;15:20417314231219280.
32. Bolon B, Carter C, Daris M, Morony S, Capparelli C, Hsieh A, Mao M, Kostenuik P, Dunstan CR, Lacey DL, Sheng JZ. Adenoviral delivery of osteoprotegerin ameliorates bone resorption in a mouse ovariectomy model of osteoporosis. Mol Ther. 2001;3(2):197-205.

33. Bellino FL. Nonprimate animal models of menopause: workshop report. Menopause. 2000;7(1):14-24.
34. Wang Z, Li X, Yang J, Gong Y, Zhang H, Qiu X, Liu Y, Zhou C, Chen Y, Greenbaum J, Cheng L, Hu Y, Xie J, Yang X, Li Y, Schiller MR, Chen Y, Tan L, Tang SY, Shen H, Xiao HM, Deng HW. Single-cell RNA sequencing deconvolutes the *in vivo* heterogeneity of human bone marrow-derived mesenchymal stem cells. Int J Biol Sci. 2021;17(15):4192-4206.
35. Liang B, Burley G, Lin S, Shi YC. Osteoporosis pathogenesis and treatment: existing and emerging avenues. Cell Mol Biol Lett. 2022;27(1):72.
36. Drake MT, Clarke BL, Khosla S. Bisphosphonates: mechanism of action and role in clinical practice. Mayo Clin Proc. 2008;83(9):1032-45.
37. Deeks ED. Denosumab: A Review in Postmenopausal Osteoporosis. Drugs Aging. 2018;35(2):163-173.
38. Anagnostis P, Paschou SA, Mintziori G, Ceausu I, Depypere H, Lambrinoudaki I, Mueck A, Pérez-López FR, Rees M, Senturk LM, Simoncini T, Stevenson JC, Stute P, Trémollieres FA, Goulis DG. Drug holidays from bisphosphonates and denosumab in postmenopausal osteoporosis: EMAS position statement. Maturitas. 2017;101:23-30.
39. Samarel AM, Ferguson AG, Decker RS, Lesch M. Effects of cysteine protease inhibitors on rabbit cathepsin D maturation. Am J Physiol. 1989;257(6 Pt 1):C1069-79.
40. Saftig P, Hetman M, Schmahl W, Weber K, Heine L, Mossmann H, Köster A, Hess B, Evers M, von Figura K, et al. Mice deficient for the lysosomal proteinase cathepsin D exhibit progressive atrophy of the intestinal mucosa and profound destruction of lymphoid cells. EMBO J. 1995;14(15):3599-608.
41. Di YQ, Han XL, Kang XL, Wang D, Chen CH, Wang JX, Zhao XF. Autophagy triggers CTSD (cathepsin D) maturation and localization inside cells to promote apoptosis. Autophagy. 2021;17(5):1170-1192.